

# Automated Physics-Derived Code Generation for Sensor Fusion and State Estimation

Orestis Kaparounakis<sup>\*§</sup>, Vasileios Tsoutsouras<sup>†</sup>, Dimitrios Soudris<sup>\*</sup>, Phillip Stanley-Marbell<sup>†</sup>

<sup>\*</sup>*Microprocessors and Digital Systems Laboratory, National Technical University of Athens, Greece*

<sup>†</sup>*Physical Computation Laboratory, University of Cambridge, United Kingdom*

<sup>\*</sup>{orestis.kapar, dsoudris}@microlab.ntua.gr, <sup>†</sup>{vt298, phillip.stanley-marbell}@eng.cam.ac.uk

**Abstract**—We present a new method for automatically generating the implementation of state-estimation algorithms from a machine-readable specification of the physics of a sensing system and physics of its signals and signal constraints. We implement the new state-estimator code generation method as a backend to generate complete C code implementations of state estimators for both linear systems (Kalman filters) and non-linear systems (extended Kalman filters). The state estimator code generation from physics specification is completely automated and requires no manual intervention. The generated filters can incorporate an Automatic Differentiation technique which combines function evaluation and differentiation in a single process.

Using the description of physical system of a range of complexities, we generate extended Kalman filters, which we evaluate in terms of prediction accuracy using simulation traces. The results show that our automatically-generated sensor fusion and state estimation implementations provide state estimation within the same error bound as the human-written hand-optimized counterparts. We additionally quantify the code size and dynamic instruction count requirements of the generated state estimator implementations on the RISC-V architecture. The results show that our synthesized state estimation implementation employing Automatic Differentiation leads to an average improvement in the dynamic instruction count of the generated Kalman filter of 7%–16% compared to the standard differentiation technique. This improvement comes at the limited cost of an average 4.5% increase in the code size of the generated filters.

**Index Terms**—Embedded Systems, State Estimation, Kalman Filters, Program Synthesis, Compilers.

## I. INTRODUCTION

**M**ANY computing systems use data from sensors to drive control decisions. Because all measurements have some degree of measurement uncertainty and sensors are no different, computing systems that consume sensor data often use techniques ranging from averaging or filtering [1], to more sophisticated state-estimation techniques [2], [3], [4], [5], to combine the signals from multiple sensors to obtain improved noise rejection. Figure 1 shows one example system: A micro-unmanned aerial vehicle (micro-UAV) weighing 27 g whose control system comprises an ARM Cortex-M4 microcontroller with 192kB RAM [6]. The system’s flight control uses data from an inertial measurement unit for 3-axis acceleration and

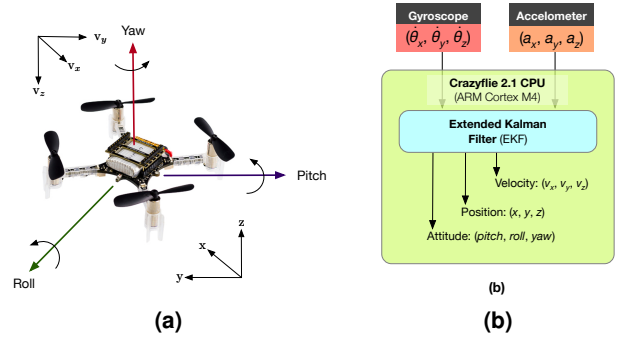


Fig. 1. (a) The CrazyFlie 2.1 micro-UAV. (b) The micro-UAV combines noisy readings from its sensors (angular rate  $\theta$  and acceleration  $a$  in three dimensions) to obtain a stable estimate of the state parameters *pitch*, *roll*, *yaw*, position  $(x, y, z)$ , and velocity  $(v_x, v_y, v_z)$ .

3-axis angular rate measurement as well as a high precision pressure sensor for elevation monitoring. The micro-UAV’s control system uses a Kalman filter to fuse the (noisy) readings from the seven dimensions of these sensors to generate a stable pitch, roll, yaw, and elevation estimate in real time [7], [8].

Implementing state-estimation methods such as Kalman filters and particle filters requires system-specific knowledge of the physical properties of the sensor-instrumented system [9]. Their implementations also typically require system-specific knowledge of the constraints imposed by physics on sensor signals. When implementing state estimation methods on resource-constrained embedded systems, this knowledge of the physics of the system is however just one part of the challenge: System designers must combine their physical understanding with efficient implementations of the core linear-algebraic methods or nonlinear dynamical systems, often in a low-level language such as C, for a hardware platform that has only tens or hundreds of kilobytes of memory and thus may not be able to host common libraries such as Eigen [10]. As a result, state estimation algorithms for resource-constrained embedded systems are challenging to implement correctly, challenging to implement efficiently, and even more challenging to implement quickly. And, because the implementations of state estimation algorithms can depend on the physical properties of a system and its sensors in complex ways, small changes to the underlying assumptions of the state estimation algorithms can require significant changes to the state estimation algorithms and their implementation.

<sup>§</sup>This work started when O. Kaparounakis was at the University of Cambridge.

This research is supported by an Alan Turing Institute award TU/B/000096 under EPSRC grant EP/N510129/1, by EPSRC grant EP/R022534/1, and by EPSRC grant EP/V004654/1.

### A. Physics-Derived State Estimator Synthesis

The behavior of physical systems deviates from the intended behavior with time (*process noise*) and measurements of signals which influence the state of a system will always have some degree of measurement uncertainty (*measurement noise*). State estimation methods estimate the future behavior or state of a system in the presence of process noise and measurement noise. In the absence of process noise, a fixed time-independent model of a system's behavior would suffice. Similarly, in the absence of measurement noise and given a model of system state as a function of external signals, one could estimate state perfectly. State estimation methods use a combination of models of the dynamics of a system and models of the noise in the system to calculate improved estimates of state variables in the presence of process noise and measurement noise.

**Key insight:** The key insight of this work is that we can use a succinct description of the physical and noise properties of a system, specified in a recently-developed physics description language [11], combined with methods recently-developed in the machine learning community for Automatic Differentiation of arithmetic expressions from representations of their abstract syntax trees (ASTs) [12], [13], within a compiler.

### B. Contributions

This article makes three key contributions to the state of the art in state estimation, code generation for embedded systems, and program synthesis. We present:

- ❶ **A new method for automated extended Kalman filter (EKF) synthesis**, with and without Automatic Differentiation (Section III).
- ❷ **An implementation of the method, including employing Automatic Differentiation within the synthesized state estimators**, for extended Backus-Naur form (EBNF) [14] expressions (Section IV).
- ❸ **An evaluation of the static and runtime behavior of the EKF state estimators that our method synthesizes** and evaluation of the benefits of Automatic Differentiation across embedded processor architectures with and with hardware support for multiplication and with and without support for single- and double-precision floating-point arithmetic, based on the RISC-V architecture (Section V).

## II. MATHEMATICAL FOUNDATION

The three central concepts in state estimation are that of a system's *state*, the system's dynamics or *process*, and *measurements*.

For example, for an unmanned aerial vehicle (UAV), the state might comprise the pitch, roll, yaw, position in three-dimensional space and velocity, as Figure 1, shown previously, illustrates. The process of the UAV represents the underlying dynamics of a system such as how its state variables vary with time. Similarly, the measurements in the UAV example are the acceleration of the UAV, measured for example using MEMS accelerometer integrated circuits integrated into the UAV hardware, or the angular rotational rate, measured for example using MEMS gyroscope integrated circuits integrated

into the UAV hardware. Even if the UAV moves according to some pre-defined flight path, its actual flight path (the process) will differ from its planned flight path. In practice, the UAV uses measurements from its sensors to estimate its current process state (pitch, roll, yaw, location, and velocity), but doing so in the presence of deviations from its planned flight path (e.g., due to cross winds) and in the presence of noisy readings from its accelerometer and gyro sensors is challenging.

The Kalman filter [2] is one method to estimate the state of a dynamic system from noisy measurements of signals that are related to the state being estimated. It works by iterating between making predictions based on current estimates and updating current estimates based on new (noisy) measurements. This iterative nature of its equations allows it to be deployed in real-time systems, continuously integrating new measurements.

### A. Notation

We notate matrices in an uppercase math boldface font (e.g., matrix  $\mathbf{H}$ ) and vectors in a lowercase math boldface font (e.g.,  $\mathbf{v}$ ). We notate all scalar variables in a standard math italic font (e.g.,  $k$ ) and scalar constants (e.g., cardinalities) in an uppercase standard math italic font (e.g.,  $N$ ). We notate estimates with a cap (e.g.,  $\hat{s}_k$ ) and the prior, previously-known, or *a priori* assumptions with a  $-$  superscript (e.g.,  $\hat{s}_k^-$ ).

Let the state of the system being modeled be denoted with vector  $\mathbf{s}$  of cardinality  $N$  and let  $k$  be an index in time. Over time, the state of a system will invariably change across time steps and we define  $\mathbf{s}_k$  as the state vector at time index  $k$ . Let  $\mathbf{F}$  be the  $N \times N$  *state transition matrix*, a matrix that describes the transformations of state across time steps.

Many systems have an ability to influence their state (e.g., by controlling motors that determine their propulsion). Let vector  $\mathbf{u}_k$  be the vector of controllable parameters of the system, with cardinality  $U$ , at time step  $k$ . Knowledge of these controllable parameters is useful in state estimation if available, but is not essential to most state estimation methods. Let  $\mathbf{B}$  be the  $N \times U$  matrix that scales the elements of the *controllable parameter vector* or *control vector*  $\mathbf{u}_k$ . In a system for which these controllable parameters are not known,  $\mathbf{B}$  is not used. For example, in a land vehicle where we can measure the angular rate of wheels but where we cannot measure the linear velocity of the vehicle, the matrix  $\mathbf{B}$  would be the transform mapping from wheel rotation rate to velocity.

Let  $\mathbf{n}_{p,k}$  be the noise vector with cardinality  $N$  (in a system with  $N$  process states) in a process at time step  $k$  and let  $\mathbf{n}_{m,k}$  be the noise vector of cardinality  $Z$  (in a system with  $Z$  sensors), at time step  $k$ . Let  $\mathbf{z}_k$  be the vector of cardinality  $Z$  comprising the estimates of the true underlying signals being measured by sensors, based on the current state and the assumption of the measurement noise. If there was no noise term in Equation 2, then one could estimate the state  $\mathbf{s}_k$  directly as the product of the inverse of  $\mathbf{H}$  and the measurement  $\mathbf{z}_k$ .

In this work, we derive  $\mathbf{F}$  and  $\mathbf{H}$  of Equations 3 and 4 from a machine-readable description of the system.

### B. Linear Kalman Filter

The simplest form of the Kalman filter is the linear Kalman filter (LKF), where the dynamic process and measurement

TABLE I

LINEAR KALMAN FILTER EQUATIONS. THE METHOD WE PRESENT IN SECTION III EXTRACTS THE INFORMATION IN THE TERMS RELATED TO THE PHYSICS OF THE SYSTEM AS WELL AS PROPERTIES OF THE NOISE WHEN PROVIDED IN THE INPUT TO THE METHOD.

<b>Process:</b>	$\mathbf{s}_k = \mathbf{F}\mathbf{s}_{k-1} + \mathbf{B}\mathbf{u}_k + \mathbf{n}_{p,k}$	(1)
<b>Measure:</b>	$\mathbf{z}_k = \mathbf{H}\mathbf{s}_k + \mathbf{n}_{m,k}$	(2)
<b>Predict:</b>	$\hat{\mathbf{s}}_k^- = \mathbf{F}\hat{\mathbf{s}}_{k-1} + \mathbf{B}\mathbf{u}_k$	(3)
	$\mathbf{P}_k^- = \mathbf{F}\mathbf{P}_{k-1}\mathbf{F}^\top + \mathbf{Q}$	(4)
<b>Gain:</b>	$\mathbf{K}_k = \mathbf{P}_k^- \mathbf{H}^\top (\mathbf{H}\mathbf{P}_k^- \mathbf{H}^\top + \mathbf{R})^{-1}$	(5)
<b>Update:</b>	$\hat{\mathbf{s}}_k = \hat{\mathbf{s}}_k^- + \mathbf{K}_k(\mathbf{z}_k - \mathbf{H}\hat{\mathbf{s}}_k^-)$	(6)
	$\mathbf{P}_k = (\mathbf{I} - \mathbf{K}_k\mathbf{H})\mathbf{P}_k^-$	(7)

functions are described by linear equations. A key insight of the LKF is that it incorporates prior information (a model) about the properties of the physical system that state variables represent. This prior information on the state vector and control vector enable the Kalman filter to predict both the state and the inter-state-variable covariance while capturing the uncertainty.

Let  $\mathbf{H}$  be the  $Z \times N$  measurement matrix, let  $\mathbf{P}$  be the  $N \times N$  state estimate covariance matrix, let  $\mathbf{Q}$  be the  $N \times N$  process uncertainty matrix, let  $\mathbf{R}$  be the  $Z \times Z$  measurement uncertainty matrix, and let  $\mathbf{K}$  be an  $N \times Z$  matrix.

**Intuition:**  $\mathbf{K}$  represents the comparison between the current covariance and the measurement noise matrix. The smaller the entries in the process uncertainty matrix  $\mathbf{Q}$ , the more the filter favors the current state. The larger the covariances in the matrix  $\mathbf{P}$  and the smaller the measurement uncertainty (entries in the matrix  $\mathbf{R}$ ), the more the Kalman filter favors the measurements. In the limit as the entries in the covariance matrix  $\mathbf{P}$  approach zero, the Kalman gain matrix  $\mathbf{K}$  approaches  $\mathbf{H}^{-1}$  therefore, the new state is based only on the prior of the physics model. Similarly, in the limit when all the entries in  $\mathbf{R}$  approach 0, the new state will be based entirely on measurements.

Table I summarizes the equations of the linear Kalman filter. The equations in Table I show the simple idea of maintaining a state estimate, updating it on new measurements according to a gain  $\mathbf{K}_k$ , that is determined by comparing our faith in our current estimates with the uncertainty of the measurements. Equations 1 and 2 correspond to the noisy process and measurement models of the system. The terms  $\mathbf{n}_{p,k}$  and  $\mathbf{n}_{m,k}$  are the zero-mean white noise for the process and the measurement model, respectively. Equations 3 and 4 formulate the prediction step, in which we propagate our current estimates of the state and its covariance through the process model. Equations 6 and 7 update the state and its covariance based on new measurements and the Kalman gain, calculated using Equation 5.

**Input of the Kalman filter:** In a linear Kalman filter the state-space is usually represented as a set of matrices, with  $N$ ,

TABLE II

EXTENDED KALMAN FILTER EQUATIONS. THE AUTOMATIC DIFFERENTIATION METHOD PRESENTED IN SECTION III-D AUTOMATES THE PROCESS OF DETERMINING THE JACOBIANS OF THE FUNCTIONS  $f$  AND  $h$ .

<b>Process:</b>	$\mathbf{s}_k = f(\mathbf{s}_{k-1}, \mathbf{u}_k) + \mathbf{n}_{p,k}$	(8)
<b>Measure:</b>	$\mathbf{z}_k = h(\mathbf{s}_k) + \mathbf{n}_{m,k}$	(9)
<b>Predict:</b>	$\hat{\mathbf{s}}_k^- = f(\hat{\mathbf{s}}_{k-1}, \mathbf{u}_k)$	(10)
<b>Update:</b>	$\hat{\mathbf{s}}_k = \hat{\mathbf{s}}_k^- + \mathbf{K}_k(\mathbf{z}_k - h(\hat{\mathbf{s}}_k^-))$	(11)

$Z$ , and  $U$  being the dimensions of the state vector, measurement vector, and input vector, respectively. The inputs of the system in this case are:

- ①  $\mathbf{F}$ : State transition  $N \times N$  matrix.
- ②  $\mathbf{H}$ : Measurement  $Z \times N$  matrix.
- ③  $\mathbf{s}_0$ : Initial state estimate  $N \times 1$  vector.
- ④  $\mathbf{P}_0$ : Initial state estimate covariance  $N \times N$  matrix.
- ⑤  $\mathbf{B}$ : Control transition  $N \times U$  matrix.
- ⑥  $\mathbf{Q}$ : Process uncertainty  $N \times N$  matrix.
- ⑦  $\mathbf{R}$ : Measurement uncertainty  $Z \times Z$  matrix.

Of these,  $\mathbf{F}$  and  $\mathbf{H}$  are crucial to describing the model of the system because the filter equations need a way to propagate the state (achieved via  $\mathbf{F}$ ) and to correlate sensor readings with the predicted state (achieved via  $\mathbf{H}$ ). The process and measurement noise may be known from sensor descriptions or can be inferred using auto-covariance methods on sample data [15]. The drawback of automatic inference is that it is usually less accurate compared to the case where the sensor noise distributions are provided.

### C. Extended Kalman Filter

Perhaps the most widely known variant of the Kalman filter is the Extended Kalman filter (EKF), derived in an effort to extend the original linear equations for usage in non-linear systems. In EKF, the new state vector and the measurement vector result from the old state by the application of functions  $f$  and  $h$  instead of a matrix multiplication.

These functions can be non-linear, such as transcendental functions (e.g.,  $\sin$  and  $\cos$ ), which are very often useful when describing physical systems. The application of these functions mandates the adaptation of the the *predict* and *update* equations. The updated equations are summarized in Table II. For the rest of the equations the  $\mathbf{F}$  and  $\mathbf{H}$  matrices now represent the Jacobian of the functions  $f$  and  $h$  at the current state with respect to the state vector variables.

**Input of the Extended Kalman filter:** Similar to the LKF,  $N$  is the dimension of the state vector,  $Z$  is the dimension of the measurement vector,  $U$  is the dimension of the input vector, while  $dt$  denotes the time difference between two successive time transitions. Additionally, we require information on the additivity of the model uncertainties  $\mathbf{Q}$  and  $\mathbf{R}$ . The inputs in EKF case are:

- ①  $f$ : State transition function of type  $(N, U, dt) \rightarrow N$ .
- ②  $h$ : Measurement function of type  $N \rightarrow Z$ .
- ③  $s_0$ : Initial state estimate  $N \times 1$  vector.
- ④  $P_0$ : Initial state estimate covariance  $N \times N$ .
- ⑤  $Q$ : Process uncertainty  $N \times N$  matrix.
- ⑥  $R$ : Measurement uncertainty  $Z \times Z$  matrix.
- ⑦ Boolean additivity values for  $Q$  and  $R$ .

As in the LKF case,  $f$  and  $h$  are crucial to describing the model of the system.

The EKF is the *de facto* standard for state estimation in non-linear systems due to its theoretical simplicity and ease of implementation compared to other approaches [4]. Despite its popularity, it suffers from two fundamental drawbacks [16]. Firstly, it uses a first-order Taylor series expansion to locally linearize the non-linear model, and thus requires the non-linearities to be mild. Secondly, its employment requires the derivation of the Jacobian matrices of the non-linear dynamic models of the system, which, if exist at all [17], are highly impractical to compute. We overcome this impracticality, using Automatic Differentiation [12], [13] as we discuss in Section III-D.

### III. AUTOMATED PHYSICS-DERIVED STATE ESTIMATOR SYNTHESIS

Linear Kalman filters (LKFs) and extended Kalman filters (EKFs) are often employed as the state estimation algorithms in cyber-physical or embedded systems. As detailed in Section II, state estimation methods such as the LKF and EKF require an understanding and model of the dynamics of the physical system for which they are implemented. This makes the rapid implementation of state estimation and sensor fusion methods challenging, especially on resource-constrained embedded systems where both execution time and memory are at a premium. As a result, there is an unmet need for automated methods for synthesizing small-footprint implementations of state estimation such as LKFs and EKFs, in low-level languages such as C, from high-level descriptions of their measurement and process dynamics.

Recent research has shown increasing interest in the development of specification languages that allow the users to specify properties of physical systems [11], [18]. We extend the specification capabilities of the Newton language [11] to allow users to input the necessary information for the generation of Kalman filters and we implement a code generation methodology as a new backend for the Newton compiler. The resulting system provides an automated method for mapping high-level system descriptions to low-level source code that can be integrated into an embedded system.

#### A. Input Specifications

The researcher or engineer using our state estimation synthesis methodology requires a method of providing an input description of a Kalman filter according to the parameters and equations of Section II. We provide a flexible and general way of representing this information, by extending the capabilities of the Newton compiler to parse equations that describe the target physical system. This enables a unified approach for

```

1  include "NewtonBaseSignals.nt"
2
3  g : constant = 9.80665 ajf;
4
5  # Ideal pendulum
6  pendulum_process : invariant( theta : angle,
7                               dtheta : angularRate,
8                               dt      : time,
9                               L       : distance) =
10 {
11   theta ~ theta + dtheta * dt,
12   dtheta ~ dtheta - g/L * sin(theta) * dt
13 }
14
15
16 pendulum_measure : invariant( theta : angle,
17                               dtheta : angularRate,
18                               dt      : time,
19                               gyro_z  : angularRate ) =
20 {
21   gyro_z ~ dtheta
22 }
23

```

Fig. 2. Physical description equations for the process and measurement models written in Newton [11]. The pendulum process invariant is modeled after the ideal pendulum (Equation 12), derived as explained in Section III-B. The invariants' arguments list all identifiers involved in the equations, and their respective dimensions. Any identifier that is not a state or a measurement variable will be passed on to the generated functions as an extra argument.

describing both linear and non-linear models and additionally allows a user of the system to define the noise distribution of the input functions.

#### B. Example: Pendulum

As a concrete example, we examine the case of the state estimation of a vertical ideal pendulum. **Notation:** Let  $\theta$  be the angle of displacement from the resting point,  $g$  the acceleration due to gravity,  $l$  the length of the rod,  $b$  the damping constant with units of  $kg\ s^{-1}$ ,  $m$  the mass of the pendulum's bob, and  $t$  the elapsed time. Then, Equation 12 describes the dynamics of the oscillation:

$$\frac{d^2\theta}{dt^2} + \frac{b}{m} \frac{d\theta}{dt} + \frac{g}{l} \sin(\theta) = 0. \quad (12)$$

**State in the pendulum example:** We define the state of the example system as the vector of the angle  $\theta$  and the derivative  $\frac{d\theta}{dt}$ . Our goal is to generate a Kalman filter which tracks the state according to the measurements from a gyroscope attached to the mass of the pendulum. To achieve that, the user must specify the *process* and *measurement* models of the pendulum. **Input specification in the pendulum example:** Figure 2 shows the Newton description of the equations for the *process* and *measurement* models in the example system. The Newton language provides the `invariant` keyword to declare a description of the physical system, whose form remains invariant throughout the lifetime of the physical object. The `~` Newton language comparison operator allows a clause in an invariant to specify that the left and right hand sides of the operator have the same units of measure and are proportional.

The *process* model of the pendulum (`pendulum_process`) appears in a linearized form, split over two equations, in order to track  $\theta$  and its derivative separately. The first equation is a time transition for  $\theta$ , which changes by  $\frac{d\theta}{dt} dt$ . The second equation is a time transition for  $\frac{d\theta}{dt}$ , which changes by  $\frac{d^2\theta}{dt^2} dt$ , according

to Equation 12. The *measure* invariant (`pendulum_measure`) corresponds to the z axis of the sensor data captured by the gyroscope. This measurement corresponds to the angular rate of the pendulum, i.e.,  $\frac{d\theta}{dt}$ .

In the general case, we make the following assumptions regarding the input description of the target physical system:

- 1) The identifiers of the *process* model invariant and the *measurement* model invariant are specified in the input.
- 2) All the left-values of the *process* model invariant constraints are part of the state of the system and all the left-values of the *measurement* model invariant constraints are measurement variables.

### C. Code Generation Algorithm

In this step, the user-provided description of the target physical system must be processed in order to generate the source code of a Kalman filter. This code is composed of the following three functions which are essential for the correct operation of the filter:

- **filterInit():** Initializes state and state covariance.
- **filterUpdate():** Ingests the input sensor measurements and incorporates them to the current state and covariance.
- **filterPredict():** Projects the state in time according to the *process* model.

The user input Newton description is parsed by the Newton parser and converted into an abstract syntax tree (AST). This AST is the input to Algorithm 1, the Kalman filter code generation algorithm.

First, from the AST, the algorithm identifies the invariants that describe the *process* and *measurement* models (Step 1). Next (Step 2), the algorithm differentiates between variables that belong to the state versus those that belong to the measurement, as well as any extra variables that must be passed to the filter functions, according to the input specification. Next (Step 3), the algorithm generates the required data structures for the filter operation. This includes C language `struct` definitions for the core data of the filter (e.g., the current state and covariance), as well as enumerations of constant values. Based on the information gathered by the three initial steps, the algorithm identifies which structures and variables need to be initialized before the execution of the filter and thus produces the **filterInit()** function in Step 4.

Next (Step 5) the algorithm performs the operations for generating the source code of the **filterPredict()** function. The algorithm performs a linearity check in Step 5a, by examining the factors of the state variables and the functions used in the expressions. If it detects a non-linear case, it generates the required C expressions in Step 5b. In a linear case Step 5b is skipped. In Step 5c the algorithm generates the propagation matrix for the linear case or the Jacobian for the non-linear case. In Step 5d the algorithm generates the body of the Kalman filter **filterPredict()** and it connects the generated function to the results of the previous steps.

The algorithm follows a similar code generation flow in Step 6, to generate the source code of the **filterUpdate()** function. The algorithm again performs a linearity check in Step 6a, and accordingly executes Steps 6b and 6c. In Step 6d the algorithm

---

### Algorithm 1: State estimation generation algorithm

---

**Data:** AST of input Newton description

**Step 1:** Identify process and measurement model invariants.

**Step 2:** Discern state and measurement variables.

**Step 3:** Generate data required filter data structures.

**Step 4:** Generate **filterInit()** function.

**Step 5:** Generate **filterPredict()** function:

**Step 5a:** Determine linearity.

**Step 5b:** Generate state propagation functions.

**Step 5c:** Construct state propagation or Jacobian (**F**).

**Step 5d:** Generate predict step matrix operations.

**Step 6:** Generate **filterUpdate()** function:

**Step 6a:** Determine linearity.

**Step 6b:** Generate state measurement functions.

**Step 6c:** Construct state measurement or Jacobian (**H**).

**Step 6d:** Generate update step matrix operations.

---

generates the necessary matrix operations for the calculations of the **filterUpdate()** equations of the Kalman filter.

### D. Automatic Differentiation for the EKF

As mentioned in Section II-C, a considerable obstacle in the incorporation of the EKF in embedded systems arises from the need to derive the Jacobian matrices of the non-linear dynamic models of the system. We address this challenge by using Automatic Differentiation (AutoDiff), a technique that computes the derivatives of code operation using the chain rule of derivatives.

AutoDiff is neither a numerical approximation of the derivative nor a symbolic method for deriving it. It can be considered as a non-standard interpretation of a computer program where the output is an augmented computer-program that also contains the calculations for various derivatives. AutoDiff has two modes of operation: *forward mode* and *reverse mode*. Consider the expression in Equation 13 (Table III) in order to explain each mode. The preliminary step is to express the expression in Equation 13 in a static single assignment (SSA) form [19], [20] as presented in Equations 14 to 17.

**Forward mode:** In this mode the intermediate derivative of an expression with respect to one of the input variables can be calculated alongside the normal function calculation. We provide an example by showing the steps required to differentiate the expression in Equation 13 with respect to an undefined variable  $t$  (Table IV). We first produce the SSA form of the expression, as shown Equations 14 to 17. By setting  $t = x$  we can calculate  $\frac{\partial z}{\partial x}$ , assuming  $\frac{\partial y}{\partial x} = 0$ . Similarly, we can calculate  $\frac{\partial z}{\partial y}$  by setting  $t = y$ . In general,  $n$  partial derivatives can be calculated with  $n$  separate function evaluations. A small overhead incurs because the function is extended to calculate the derivatives alongside execution. The overhead for the Forward Mode is approximately  $O(n)$ , where  $n$  is the number of operations in the original function.

**Reverse mode:** In this mode, the calculation of the output of the function takes place first, untangled from the calculations for the partial derivatives. Afterwards, the partial derivatives of the output with respect to each intermediate result are calculated downwards, in a fountain-like manner, until those with respect to each input variable are reached. Starting from Equation 17, the final assignment of the SSA form of the

TABLE III  
EXAMPLE EXPRESSION AND ITS SSA FORM CODE SEQUENCE

Original	SSA Form
$z = x * y^2 + \sin(x).$ (13)	$r_1 = y^2;$ (14)
	$r_2 = x \cdot r_1;$ (15)
	$r_3 = \sin(x);$ (16)
	$z = r_2 + r_3.$ (17)

expression in Equation 13 we differentiate an undefined variable  $s$  with respect to each one of the left values in Equations 14 to 16, i.e.,  $r_1$  to  $r_3$ . This can be perceived as finding out what output variables a given input variable can affect and by how much. The updated expressions are provided in Table IV. By setting  $s = z$  we get both  $\frac{\partial z}{\partial x}$  and  $\frac{\partial z}{\partial y}$  in the same run. As a result,  $n$  partial derivatives can be calculated with one function evaluation and a small overhead due to the computation of the partial derivatives. The computational overhead, similarly to Forward Mode, is roughly  $O(n)$ , but Reverse Mode needs memory space proportional to the complexity of the original function for storing intermediate values.

The Forward Mode AutoDiff is able to calculate the partial derivatives of all the output variables with respect to one input variable in the same pass, whereas in Reverse Mode AutoDiff we can calculate the partial derivatives of one output variable with respect to all input variables in the same pass. In the context of calculating the Jacobian, Forward Mode computes columns while Reverse Mode computes rows. As such, with AutoDiff, a precise calculation of the Jacobian can be performed in  $n$  evaluations of the original function [12], [13]. In our case the user inputs the model as a series of equations, one for each output variable. For this, it is more convenient to implement the Reverse Mode.

The AutoDiff engine was implemented as compiler back-end and uses a three-pass method to annotate the AST nodes and then generate the output code. In the first pass, with a pre-order traversal, each node of the tree is assigned a “variable

TABLE IV  
MODES FOR AUTOMATIC DIFFERENTIATION.

Forward Mode	Reverse Mode
$\frac{\partial r_1}{\partial t} = 2 \cdot \frac{\partial y}{\partial t}$ (18)	$\frac{\partial s}{\partial r_3} = \frac{\partial s}{\partial z}$ (19)
$\frac{\partial r_2}{\partial t} = x \cdot \frac{\partial r_1}{\partial t} + r_1 \cdot \frac{\partial x}{\partial t}$ (20)	$\frac{\partial s}{\partial r_2} = \frac{\partial s}{\partial z}$ (21)
$\frac{\partial r_3}{\partial t} = \cos(x) \cdot \frac{\partial x}{\partial t}$ (22)	$\frac{\partial s}{\partial r_1} = x \cdot \frac{\partial s}{\partial r_2}$ (23)
$\frac{\partial z}{\partial t} = \frac{\partial r_2}{\partial t} + \frac{\partial r_3}{\partial t}$ (24)	$\frac{\partial s}{\partial x} = r_1 \cdot \frac{\partial s}{\partial r_2} + \cos(x) \cdot \frac{\partial s}{\partial r_3}$ (25)
	$\frac{\partial s}{\partial y} = 2 \cdot \frac{\partial s}{\partial r_1}$ (26)

identifier”. This will identify the intermediate result of this node in the SSA form. In the second pass, with a post-order traversal, the SSA form of the expression is printed to a buffer using those identifiers. In the third, with a pre-order traversal, the reverse SSA form for the calculation of the chained partial derivatives is exported.

### E. End-to-End Example

Our code generation process consists of two main stages. **Static Compile-Time Analysis** and **Dynamic Online Usage**. Figure 3 illustrates an end-to-end example of the operation and connections of all the subcomponents presented in Sections III-A to III-D, to achieve automated Kalman filter source code generation.

## IV. IMPLEMENTATION

### A. API of the Interaction with the Synthesized Filter

The output of the synthesis is the generated Kalman filter source code, either LKF or EKF, which follows the conventions presented in Section III. We instruct the synthesized source code to automatically interface the final binary against a lightweight implementation of the necessary linear algebra functions. The user also has the option to provide their own libraries.

For the case of EKF, the user can choose between Standard and Automatic Differentiation. The key differences between these in the generated code are: (i) the state and measurement equations use functions instead of matrices; (ii) the Jacobian matrix is calculated at each step using the derivatives of state and measurement functions as follows. **Standard differentiation:** Another set of  $O(N^2 + Z^2)$  functions are created for the derivative of each function with regards to each state variable. **Automatic differentiation:** The generation of the first  $O(N + Z)$  functions is hi-jacked to produce the SSA form code of the expression and the Reverse Mode AutoDiff calculation of the derivatives, detailed in III-D.

The code generation back-end outputs code fragments by traversing the AST corresponding to each user input. Reusable intermediate results are kept internally for use at subsequent steps of the code generation back-end. The source code is incrementally stored in a buffer and eventually written to a user-specified file.

### B. Newton Language: Extensions and Limitations

Support for the required constructs to model Kalman filters in the Newton language [11] grammar varies. Matrix notation is not directly supported in the grammar but expression lists inside the invariants are.

Newton implements a dimensional type system that uses signals as types (e.g. *angle*, *time* and *distance* in Fig. 2). Primitive signals (e.g. the S.I. units) are defined in the include file, *NewtonBaseSignals.nt*. Dimensions can be applied to an identifier through a signal and new signals can be declared. A Newton description must satisfy this type system, i.e. be dimensionally correct, for the compiler to accept it. This is an additional way to prevent wrong filters from being generated.

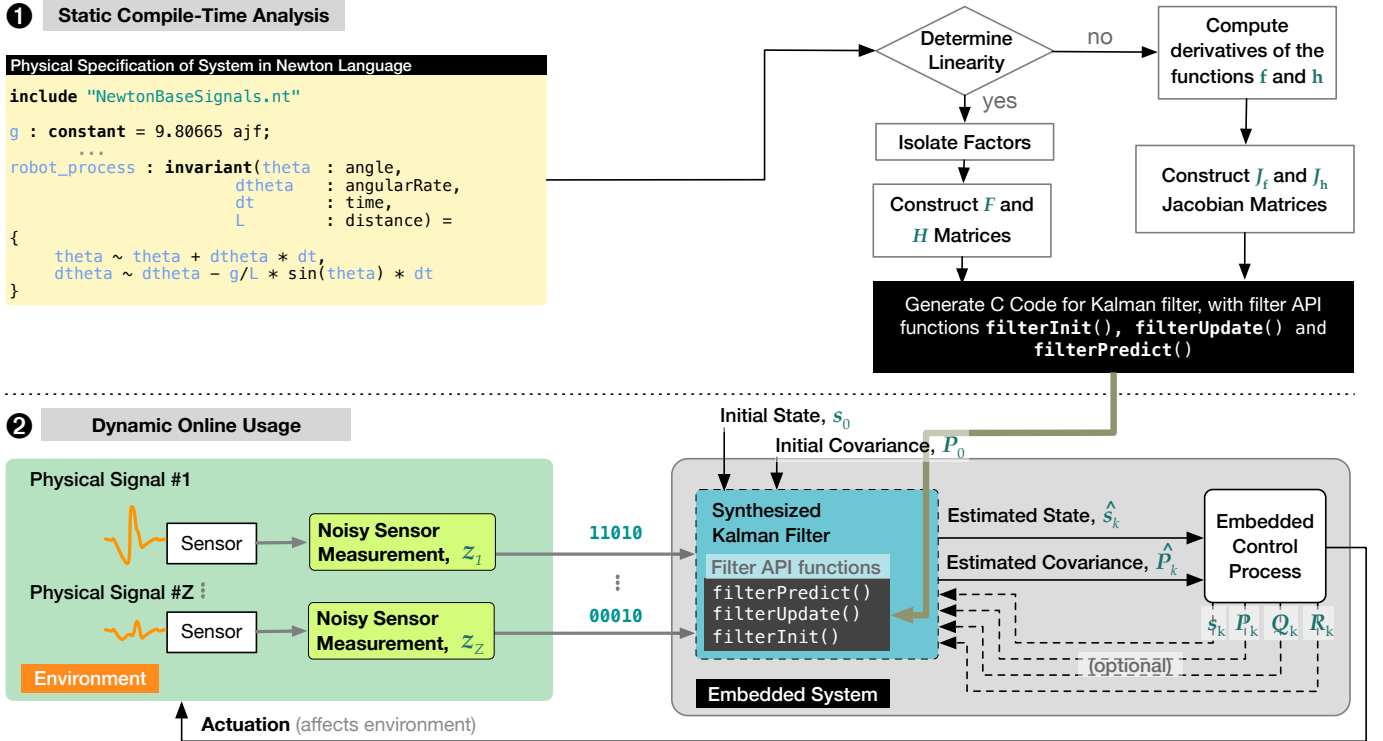


Fig. 3. System overview. In the **Static Compile-Time Analysis** stage the user provides a physical specification of the embedded system in question, encoded as an Newton language description file. The Newton compiler parses and dimensionally checks the file. The generated AST is directed to the code generation back-end which starts with a linearity check and proceeds accordingly to the generation of the expressions and the matrices required by the Kalman filter algorithm. The algorithmic steps involved in this process have been presented in Section III-C. In the **Dynamic Online Usage** stage the user evaluates the synthesized Kalman filter either in simulation or in the actual target embedded systems. The run-time stage of the filter commences with the initialization of the state and covariance. When the target computing system establishes its interaction with the physical environment, the prediction and update functions of the Kalman filter are invoked according to the target application control flow. The dynamically estimated state and covariance are available to any scope that can access the core data structures of the filter. An optional injection of a state is also supported.

Uncertainty notation is implemented as an extension of the signal declaration statement. Any signal can be optionally enhanced with uncertainty information by providing the expected distribution and its parameters as an argument. In the context of this work we have only worked with Gaussian distributions, but the compiler can be extended in a straightforward manner to support other distributions.

The engine for Automatic Differentiation (Section III-D) of Newton expressions was implemented as a three-pass algorithm of the compiler AST. By design, it is abstracted from the estimator generation back-end, making the technique available to any code generation back-end or other compiler with similar AST structure.

## V. EXPERIMENTAL EVALUATION

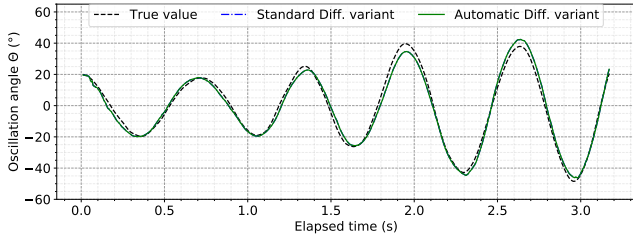
### A. Pendulum System

In our first experiments we target the problem of state estimation of a physical system which simulates the oscillation of an ideal pendulum. The dynamics of the oscillation are presented in Equation 12.

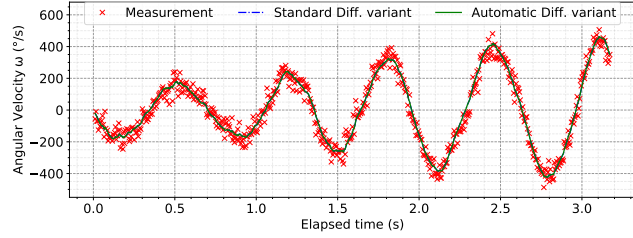
We developed Newton descriptions similar to the one presented in Figure 2 to describe the pendulum with and without drag in order to use our implemented Newton compiler back-end for the generation of Kalman filters. The state vector of the system is  $\langle \theta_t, \omega_t \rangle$ , composed of the oscillation angle

and the angular velocity, respectively. The input of the filters is the angular velocity provided by a simulated gyroscope. The measurements from the gyroscope are noisy and the noise was modelled, without lack of generality, according to a Gaussian distribution. The angular rate of the gyroscope is the only sensory input to the generated Kalman filters, which are completely agnostic to the deviation of the estimated angle from the true one. We generated two different variants of the filter, one that uses standard differentiation and one that uses Automatic Differentiation.

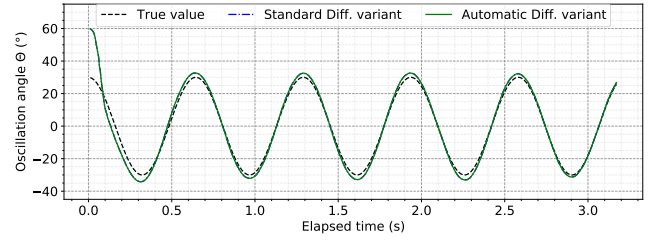
We first evaluate a pendulum without drag, using its dynamics equation to simulate its oscillation in time and gather a trace of the state and sensor values. We then use the generated Kalman filters to predict the time-evolution of the pendulum state parameters in the presence of noisy input sensor measurements. Figures 4(a) and 4(c) present an execution interval of the simulation, with initial pendulum displacement of  $20^\circ$  and observable process noise of variance  $0.005 \text{ rad}^2/\text{s}^2$  on the angular velocity  $\omega$ . The sensor error distribution has zero mean value and variance equal to  $0.5 \text{ rad}^2/\text{s}^2$ . The sensed values from the gyroscope are annotated in Figure 4(c) with red points, combined with the pendulum angular velocity predicted by the two Kalman filter variants. In Figure 4(c), we provide the predicted pendulum angle by the two Kalman filters compared against the true value. We observe that both filter variants



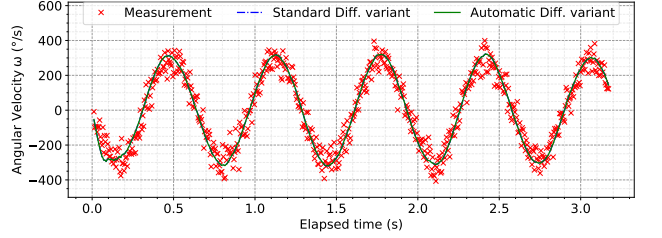
(a) Experiment 1: Estimation of oscillation angle over time.



(c) Experiment 1: Estimation of angular velocity over time.



(b) Experiment 2: Estimation of oscillation angle over time.



(d) Experiment 2: Estimation of angular velocity over time.

Fig. 4. Evaluation of generated Kalman filter for estimation of the state a pendulum. Sub-figures (a) and (c) correspond to an oscillation with initial displacement of  $20^\circ$  and observable process noise of variance  $0.005 \text{ rad}^2/\text{s}^2$  in the angular velocity  $\omega$  of the oscillation (notice the changes in maximum amplitude and frequency). The input to the filters is angular velocity from a gyro with noise of variance  $0.5 \text{ rad}^2/\text{s}^2$ . All generated filter variants manage to follow the noisy process with a mean square error of  $0.0025 \text{ rad}^2$  for the angle and  $0.17 \text{ rad}^2/\text{s}^2$  for the angular velocity. Sub-figures (b) and (d) correspond to a different pendulum simulation with initial displacement of  $30^\circ$ , measurement noise of variance  $0.8 \text{ rad}^2/\text{s}^2$ . Examined filters were deliberately erroneously initialized with the knowledge of an initial displacement of  $60^\circ$ . Nevertheless, they manage to converge to accurate estimations about the state of the pendulum.

are capable of correctly estimating the oscillation with mean square error (MSE) of  $0.003 \text{ rad}^2$ .

In our second experiment using the pendulum with no drag, we initialize the generated Kalman filters with a “false” initial angle displacement value. In this way, we evaluate their ability to estimate the state of the system when the initial state information are not accurate. The initial displacement was set to  $30^\circ$ , while the filters were initialized with knowledge of  $60^\circ$  displacement. We provide the results of this experiment in Figure 4(b) and Figure 4(d). We observe in Figure 4(b) that both filter variants are capable of converging to accurate predictions of the system’s state. For both filters, the MSE of the prediction of the oscillation angle  $\theta$  was  $0.0056 \text{ rad}^2$ , while the MSE value for the prediction of the angular rate  $\omega$  was  $0.1757 \text{ rad}^2/\text{s}^2$ .

We performed a third experiment for the state estimation of a pendulum with drag, length equal to  $0.5 \text{ m}$  and damping factor equal to  $0.8 \text{ kg s}^{-1}$ . The initial angle displacement was  $30^\circ$  and both filter variants were provided correct information about this value. The results of this experiment are shown in Figure 5. The measurement noise variance was  $0.8 \text{ rad}^2/\text{s}^2$ . We observe that both Kalman filter variants are capable of making accurate predictions about the system state, despite the noise in measurements, annotated with red points in Figure 5(b). The MSE of the prediction for both filters was approximately  $0.0002 \text{ rad}^2$  for the prediction of the oscillation angle  $\theta$  and  $0.0054 \text{ rad}^2/\text{s}^2$  for the prediction of the angular rate  $\omega$ .

## B. TurtleBot3 Robot

To evaluate the effectiveness of the generated filters on the state estimation of a complex cyber-physical system, we make use of the TurtleBot3 Burger [21], a robot built on open-source

software. The TurtleBot3 Burger is a differential drive robot, i.e., it controls its linear and angular velocities by actuating on a set of wheels with individual speed setpoints  $v_r$  and  $v_l$ , for the right and the left wheel, respectively. The general kinematic model of such a robot exhibits a non-holonomic constraint and thus the process model, described by Dudek et al. [22], is split in two special cases:

If  $v_r = v_l = v$ :

$$\begin{bmatrix} x_{t+\delta t} \\ y_{t+\delta t} \\ \theta_{t+\delta t} \end{bmatrix} = \begin{bmatrix} x_t + v \cos(\theta_t)\delta t \\ y_t + v \sin(\theta_t)\delta t \\ \theta_t \end{bmatrix} \quad (27)$$

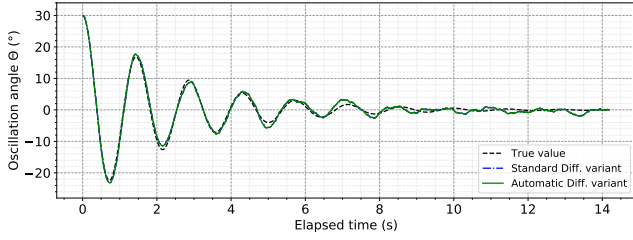
and if  $v_r = -v_l = v$ :

$$\begin{bmatrix} x_{t+\delta t} \\ y_{t+\delta t} \\ \theta_{t+\delta t} \end{bmatrix} = \begin{bmatrix} x_t \\ y_t \\ \theta_t + 2v\delta t/l \end{bmatrix} \quad (28)$$

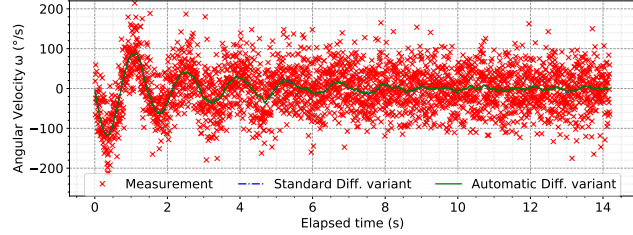
where  $x$ ,  $y$  and  $\theta$  are the robot’s position and yaw in the fixed frame,  $v$  is the velocity in the fixed frame,  $\delta t$  is the time difference between subsequent runs of the model and  $l$  is the distance between the two wheels. The subscript denotes a given point in time  $t$ .

We generated the robot process Newton invariant as a unified model and hardcoded a C control flow command in the generated *Predict* function to check the system’s input, i.e. the velocities  $v_r$ ,  $v_l$ , and perform the correct operations according to either Equation 27 or Equation 28. We instructed the measurement model to use the IMU and simulated localization information from laser scanners of the robot. This information is treated as noisy information on the robot’s position on the  $XY$  plane, with variance  $0.1 \text{ m}^2$  for both directions. We simulated a stroll of the robot on the Gazebo [23] simulation platform and recorded the sensor measurements trace.





(a) Estimation of oscillation angle over time.



(b) Estimation of angular velocity over time.

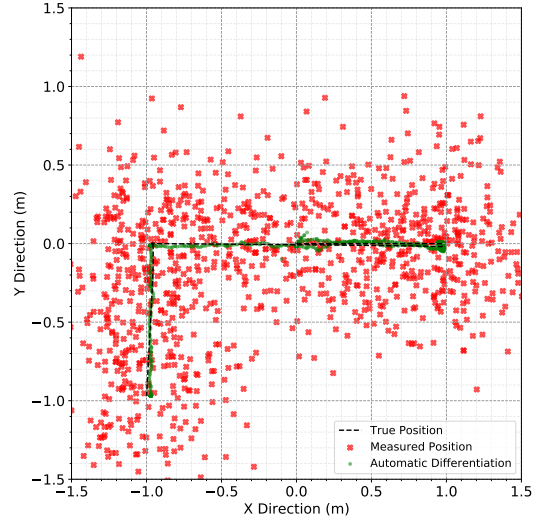
Fig. 5. State estimation of a pendulum oscillation with drag. Initial displacement is equal to  $30^\circ$  and measurement noise variance  $0.8 \text{ rad}^2/\text{s}^2$ . Both generated filter variants, i.e., with standard or Automatic Differentiation, provide high accuracy estimates of the oscillation with diminishing amplitude.

We utilized the recorded trace to evaluate the effectiveness of our generated Kalman filter with Automatic Differentiation in predicting the state vector  $\langle x_t, y_t, \theta_t \rangle$  of the robot. Figure 6 presents the estimation results for the position (Figure 6(a)) and yaw (Figure 6(b)) of the robot, both represented using green lines. The recorded measurements from the sensor of the robot are annotated in Figure 6(a) with red points. The robot started its stroll at position  $(0, 0)$  facing towards the positive side of the x axis. We instructed it to move straight to position  $(1, 0)$ , turn  $180^\circ$  right, continue to  $(-1, 0)$ , turn  $90^\circ$  left and finish its movement at position  $(-1, -1)$ . The dashed black line in Figure 6(a) corresponds to the actual trajectory of the robot and we can observe the high estimation accuracy of our generated Kalman filter, despite the noise in the measured values. The average Euclidean error of the translational movement of the robot is  $0.0185 \text{ m}$  whereas the average error of the rotational movement (Figure 6(b)) is  $4.72^\circ$ .

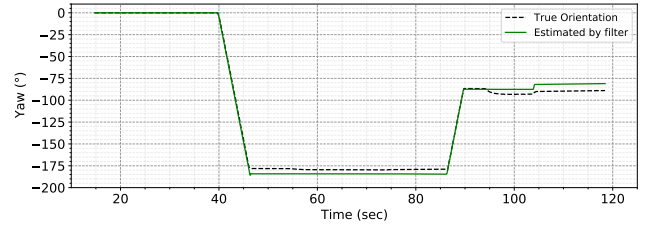
### C. Code Size & Performance Evaluation

Additionally to evaluating the accuracy of the generated filters, it is also important to quantify their memory and computational requirements. Thus, we profiled the generated filters for state estimation of a pendulum without drag, as presented in Section V-A. We choose RISC-V as the target reference 32-bit RISC CPU architecture and examine different extensions of the instruction set architecture (ISA) to take into account embedded systems of different computational competency. Starting from the RV32I base integer ISA, which provides only integer addition/logical operations, we also examine RV32IM extension with integer multiplication and division instructions and RV32IMF/RV32IMFD extensions for single/double precision floating-point arithmetic operations.

The generated Kalman filter source code contains double precision variables and has been compiled using GCC 8.2.0.



(a) Actual path and path estimation of TurtleBot3.



(b) Rotational movement estimation of TurtleBot3 using a gyroscope.

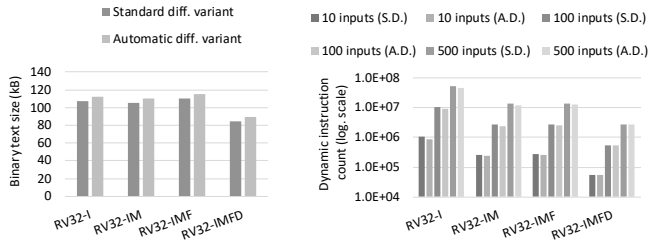
Fig. 6. Prediction of the path of the TurtleBot3 Burger robot. It starts at position  $(0, 0)$  facing the positive values of x axis. It moves straight to  $(1, 0)$ , turns  $180^\circ$  left, continues to  $(-1, 0)$ , turns  $90^\circ$  left and finally moves to  $(-1, -1)$  as shown in Sub-figure (a). Sub-figure (b) shows the actual and estimated value of the yaw of the robot using a generated Kalman filter.

We examined both variants of standard and Automatic Differentiation and benchmarked the generated filters for an increasing amount of input workload by varying the amount of total sensor inputs that are being processed for estimation of the state. For this experiment, we examine inputs of 10, 100 and 500 sensor measurements of the angular rate  $\omega$  of the pendulum.

Both filters were compiled with the '-O3' optimization option and we evaluated the binary size of the generated Kalman filters using the *riscv32-elf-size* tool. We additionally evaluated the dynamic instruction count for the execution of the Kalman filters using Sunflower [24], an open-source embedded system micro-architectural emulator. The input sensor samples have been hardcoded in the source in order to decouple our measurements from the required instructions for disk I/O.

The size of the 'text' segment of the filter binaries, for the different ISA extensions is illustrated in Figure 7(a). The dynamic instructions count for the completion of the filters' execution for varying input size is presented in Figure 7(b). Standard and Automatic Differentiation filter variants are annotated using 'S.D.' and 'A.D.', respectively. Each bar of Figure 7(b) corresponds to a different workload, i.e. different total number of input sensor vectors processed by the filter.

We observe that in all cases the filter variant with Automatic Differentiation is slightly larger in size but requires less



(a) Binary text size in kB. (b) Dyn. instruction count (log scale).

Fig. 7. Profiling of the compiled binaries of the generated filters’ source code for various RISC-V ISA extensions. Sub-figure (a) shows the size of the ‘text’ segment of the binaries, showing a slight increase for filters with Automatic Differentiation. Sub-figure (b) shows the required instructions for the processing of input sensor vectors, where the filters with Automatic Differentiation achieve significant reduction compared to standard differentiation.

instructions for its completion (note that the Y-axis scale of Figure 7(b) is logarithmic). Automatic differentiation results in an average gain of more than 7.5% in the required instructions for the filter execution, exceeding 16% at its maximum in the case of RV32I ISA. The tradeoff is an average increase of 4.7% in the ‘text’ segment of the compiled binary.

We attribute the increase in ‘text’ size to (i) the expansions of the Kalman filter equations to their SSA form and (ii) the inclusion of the SSA form of the Reverse Mode AutoDiff (Section III-D). The reduction of the dynamic instructions is attributed to the usage of Automatic Differentiation, which calculates the partial derivatives in the rows of the Jacobian matrices in a single function evaluation (Section IV-A). Conversely, standard differentiation needs to evaluate the required functions two times more for each partial derivative of a row.

## VI. RELATED RESEARCH

Automating Kalman filter design and implementation process is a task of high importance for engineers in various domains. As a result, MATLAB and GNU Octave both provide libraries that assist the design of Kalman filters [25], [26] and MATLAB provides the ability for automated generation of C/C++ source code for filters. A python package for Kalman filtering is also available [27], offering a range of filters and great documentation, but focusing on pedagogy rather than implementation efficiency. These solutions are either proprietary or are not directly applicable to the majority of embedded applications as these require small code size and small memory usage.

The most prominent related research is the AutoFilter [28], [29], a closed-source tool which supports code generation for the LKF, the linearized filter, and the EKF. AutoFilter offers abstractions for transformations such as linearization and transforming the system from continuous to discrete. The generated code can be in the form of C/C++, Modula-II source code, or a MATLAB script. AutoFilter relies on an input grammar, which supports the definition of constants, input data, datatypes, vectors, matrices and distributions [28]. The target model in this grammar is declared as a list of equations. This approach favors the description of non-linear models but is unintuitive in the case of linear systems. Furthermore, although

the authors claim that the tool supports differential equations, the input grammar merely equates each differential of the state variables with an algebraic expression.

AutoFilter and the automated solutions and libraries described above, all assume a static time difference between execution steps. In real-world embedded systems however, the time difference between consecutive readings from one sensor may vary and readings across multiple sensors are often at different timestamps. In contrast to all prior work, the method we present in this work makes no such assumptions about time steps. Our method exploits information about the physics of a system, is generalizable beyond Kalman filters, and builds on recent results in Automatic Differentiation [12], [13] to automate the generation of the Jacobians in the non-linear EKF.

## VII. CONCLUSION AND FUTURE WORK

This article presents an advance in the state of the art in automated synthesis of state estimation and sensor fusion algorithms. The method we present starts from a specification of the physics of an embedded sensor-driven system and its environment. It generates, as output, C code with small code and memory footprint, suitable for deployment of ultra-low-power microcontrollers. The automation of the method by its implementation within a compiler for a physics specification language reduces the time-consuming and potentially error-prone process of designing and updating state estimation algorithms such as linear and extended Kalman filters.

The method we present is easily extended to support other state estimation algorithms, such as the unscented Kalman filter and the particle filter, or different approaches to filter subcomponents, such as using an information matrix instead of a covariance matrix [30], enabling rapid comparison between multiple filter variants for the same embedded solution. Additionally, the implementation of the method within a compiler for a physical system specification language makes it possible to add more static compile-time analysis for the output system, optimizing multiple parts of the resulting code in terms of efficiency, complexity and code size as well as providing this information to the user before deployment.

Our implementation exploits recent advances in Reverse-Mode Automatic Differentiation of program sequences, borrowed from the world of machine learning, to automate the generation of the partial derivatives of the state equation for the Jacobian matrices for the extended Kalman filter. Using descriptions of physical systems of a range of complexities, we evaluate and validate the generated filters in terms of accuracy, stability, convergence, and run-time requirements for deployment in resource-constrained environments.

## REFERENCES

- [1] A. V. Oppenheim and R. W. Schaffer, “Digital signal processing. 1975,” *Englewood Cliffs, New York*, 1983.
- [2] R. Kalman, “E. 1960. a new approach to linear filtering and prediction problems,” *Transactions of the ASME—Journal of Basic Engineering*, vol. 82, pp. 35–45, 1960.
- [3] A. H. Jazwinski, “Adaptive filtering,” *Automatica*, vol. 5, no. 4, pp. 475–485, 1969.

- [4] E. A. Wan and R. Van Der Merwe, "The unscented kalman filter for nonlinear estimation," in *Proceedings of the IEEE 2000 Adaptive Systems for Signal Processing, Communications, and Control Symposium (Cat. No. 00EX373)*. Ieee, 2000, pp. 153–158.
- [5] M. S. Arulampalam, S. Maskell, N. Gordon, and T. Clapp, "A tutorial on particle filters for online nonlinear/non-gaussian bayesian tracking," *IEEE Transactions on signal processing*, vol. 50, no. 2, pp. 174–188, 2002.
- [6] W. Giernacki, M. Skwierczyński, W. Witwicki, P. Wroński, and P. Kozierski, "Crazyflie 2.0 quadrotor as a platform for research and education in robotics and control engineering," in *2017 22nd International Conference on Methods and Models in Automation and Robotics (MMAR)*. IEEE, 2017, pp. 37–42.
- [7] M. W. Mueller, M. Hamer, and R. D'Andrea, "Fusing ultra-wideband range measurements with accelerometers and rate gyroscopes for quadcopter state estimation," in *2015 IEEE International Conference on Robotics and Automation (ICRA)*, May 2015, pp. 1730–1736.
- [8] M. W. Mueller, M. Hehn, and R. D'Andrea, "Covariance correction step for kalman filtering with an attitude," *Journal of Guidance, Control, and Dynamics*, pp. 1–7, 2016.
- [9] T. D. Barfoot, *State estimation for robotics*. Cambridge University Press, 2017.
- [10] G. Guennebaud, B. Jacob *et al.*, "Eigen," *URL: http://eigen.tuxfamily.org*, 2010.
- [11] J. Lim and P. Stanley-Marbell, "Newton: A language for describing physics," *arXiv preprint arXiv:1811.04626*, 2018.
- [12] A. G. Baydin, B. A. Pearlmutter, A. A. Radul, and J. M. Siskind, "Automatic differentiation in machine learning: a survey," *The Journal of Machine Learning Research*, vol. 18, no. 1, pp. 5595–5637, 2017.
- [13] C. C. Margossian, "A review of automatic differentiation and its efficient implementation," *Wiley Interdisciplinary Reviews: Data Mining and Knowledge Discovery*, vol. 9, no. 4, p. e1305, 2019.
- [14] N. Wirth, "What can we do about the unnecessary diversity of notation for syntactic definitions?" *Commun. ACM*, vol. 20, no. 11, p. 822–823, Nov. 1977.
- [15] B. J. Odelson, M. R. Rajamani, and J. B. Rawlings, "A new autocovariance least-squares method for estimating noise covariances," *Automatica*, vol. 42, no. 2, pp. 303–308, 2006.
- [16] S. Haykin and I. Arasaratnam, "Cubature kalman filters," *IEEE Trans. Autom. Control*, vol. 54, no. 6, pp. 1254–1269, 2009.
- [17] S. J. Julier and J. K. Uhlmann, "Unscented filtering and nonlinear estimation," *Proceedings of the IEEE*, vol. 92, no. 3, pp. 401–422, 2004.
- [18] Y. Wang, S. Willis, V. Tsoutsouras, and P. Stanley-Marbell, "Deriving equations from sensor data using dimensional function synthesis," *ACM Transactions on Embedded Computing Systems (TECS)*, vol. 18, no. 5s, pp. 1–22, 2019.
- [19] B. Alpern, M. N. Wegman, and F. K. Zadeck, "Detecting equality of variables in programs," in *Proceedings of the 15th ACM SIGPLAN-SIGACT symposium on Principles of programming languages*, 1988, pp. 1–11.
- [20] M. Braun, S. Buchwald, S. Hack, R. Leißa, C. Mallon, and A. Zwinkau, "Simple and efficient construction of static single assignment form," in *International Conference on Compiler Construction*. Springer, 2013, pp. 102–122.
- [21] R. Amsters and P. Slaets, "Turtlebot 3 as a robotics education platform," in *International Conference on Robotics and Education RiE 2017*. Springer, 2019, pp. 170–181.
- [22] G. Dudek and M. Jenkin, *Computational principles of mobile robotics*. Cambridge university press, 2010.
- [23] N. Koenig and A. Howard, "Design and use paradigms for gazebo, an open-source multi-robot simulator," in *2004 IEEE/RSJ International Conference on Intelligent Robots and Systems (IROS)(IEEE Cat. No. 04CH37566)*, vol. 3. IEEE, 2004, pp. 2149–2154.
- [24] P. Stanley-Marbell and D. Marculescu, "Sunflower: Full-system, embedded microarchitecture evaluation," in *International Conference on High-Performance Embedded Architectures and Compilers*. Springer, 2007, pp. 168–182.
- [25] M. S. Grewal and A. P. Andrews, *Kalman filtering: Theory and Practice with MATLAB*. John Wiley & Sons, 2014.
- [26] S. Särkkä, *Bayesian filtering and smoothing*. Cambridge University Press, 2013, vol. 3.
- [27] R. Labbe, "Kalman and bayesian filters in python," 2015.
- [28] J. Whittle and J. Schumann, "Automating the implementation of kalman filter algorithms," *ACM Transactions on Mathematical Software (TOMS)*, vol. 30, no. 4, pp. 434–453, 2004.
- [29] J. Richardson and E. Wilson, "Flexible generation of kalman filter code," in *2006 IEEE Aerospace Conference*. IEEE, 2006, pp. 8–pp.
- [30] G. A. Terejanu, "Discrete kalman filter tutorial," *University at Buffalo, Department of Computer Science and Engineering, NY*, vol. 14260, 2013.